Article

Characterization of Oxygen Dynamics in ZrWO

Matthew R. Hampson, John S. O. Evans, and Paul Hodgkinson

J. Am. Chem. Soc., **2005**, 127 (43), 15175-15181• DOI: 10.1021/ja054063z • Publication Date (Web): 11 October 2005

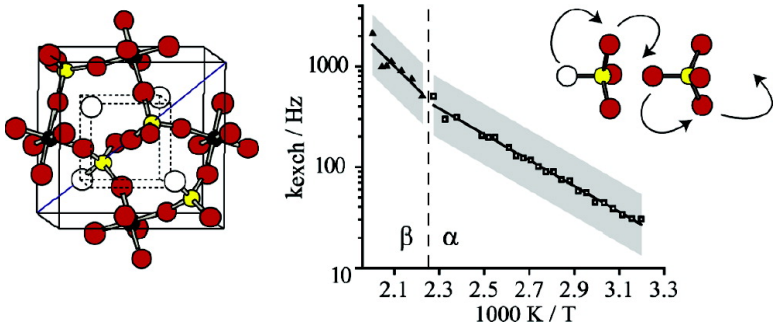

More About This Article

Additional resources and features associated with this article are available within the HTML version:

- Supporting Information
- Links to the 5 articles that cite this article, as of the time of this article download
- Access to high resolution figures
- Links to articles and content related to this article
- Copyright permission to reproduce figures and/or text from this article

View the Full Text HTML

J|A|C|S
ARTICLES
Published on Web 10/11/2005

Characterization of Oxygen Dynamics in ZrW_2O_8

Matthew R. Hampson, John S. O. Evans,* and Paul Hodgkinson*

Contribution from the Department of Chemistry, Durham University, South Road, Durham DH1 3LE, United Kingdom

Received June 20, 2005; E-mail: john.evans@durham.ac.uk; paul.hodgkinson@durham.ac.uk

Abstract: The dynamics of oxygen motion in ZrW_2O_8 have been characterized using ^{17}O solid-state NMR. Rates of dynamic exchange have been extracted from magnetization transfer experiments over a temperature range of 40 to 226 °C, and distinct values for the associated activation barrier have been observed on either side of the order/disorder phase transition at ~175 °C. A detailed model for the dynamical process is proposed, which reconciles the observation of continuing oxygen dynamics in the low-temperature phase with the static order implied by earlier X-ray diffraction studies.

Introduction

The cubic AM_2O_8 family of materials has attracted considerable attention due to the unusual phenomenon of negative thermal expansion (NTE), contracting isotropically in volume on heating from 0.2 to 1050 K.[1−3] This behavior has been linked to their unusual framework structure, which can be described as a network of corner-sharing AO_6 octahedra and MO_4 tetrahedra with the tetrahedra sharing only three of their four corners with octahedra. This leads to an inherently flexible structure that can support low-energy negative-Gruneisen-parameter modes, which tend to contract the material.[4,5] The structure determined by powder diffraction, shown in Figure 1a, contains four crystallographically unique oxygen sites.[1,6] The WO_4 tetrahedra are arranged in pairs that lie on the 3-fold axes of its cubic cell, and the O1 and O2 sites (part of Zr−O−W linkages) are crystallographically inequivalent, although in chemically similar environments. The "terminal" oxygens of each WO_4 point in the same direction, leading to a O4−W1···O3−W2 arrangement in which O4 is strictly one coordinate (Figure 1b). Diffraction studies have shown that the WO_4 pairs are ordered at low temperature, leading to an acentric space group ($P2_13$) for the α phase. Above ~175 °C, however, these groups become dynamically disordered over two possible orientations in the unit cell ($W-O_{terminal}$ vectors pointing along both (x, x, x) and $(-x, -x, -x)$ and equivalent directions), such that the time-averaged structure of the β phase adopts the centrosymmetric space group $Pa\bar{3}$. There is strong evidence from diffraction data that dynamic disorder of this type occurs at temperatures as low as ~200 K in the related materials $ZrWMoO_8$ and $ZrMo_2O_8$.[7,8] Significant oxygen mobility at low temperatures in the solid state is unusual,[9] but has been observed, for example, in materials with excess oxygen, such as those related to the high-temperature cuprate superconductors, including $La_2CuO_{4+\delta}$[10−12] and $La_2NiO_{4+\delta}$.[9,13,14] Insight into the mechanism and structural origin of oxygen mobility in ZrW_2O_8 may provide fundamental new insight in the search for new ionic conductors.

Although diffraction studies are invaluable in providing the average structure of the material, information about oxygen dynamics is provided only indirectly. In the high-temperature phase, for example, the X-ray diffraction data show that the W_2O_8 units are randomly ordered, but do not reveal whether this disorder is static or dynamic. In contrast, ^{17}O solid-state NMR[15] provides localized information on the oxygen sites, and so is strongly complementary to long-range information from diffraction studies. Crystalline ionic materials are well suited to ^{17}O studies, since the broadenings due to quadrupolar coupling are modest, allowing relatively small chemical shift differences to be resolved.[16] ^{17}O NMR is particularly useful in the characterization of dynamic processes.[17−21] In the case of

(1) Mary, T. A.; Evans, J. S. O.; Vogt, T.; Sleight, A. W. *Science* **1996**, *272*, 90−92.
(2) Evans, J. S. O.; Mary, T. A.; Vogt, T.; Subramanian, M. A.; Sleight, A. W. *Chem. Mater.* **1996**, *8*, 2809−2823.
(3) Evans, J. S. O.; David, W. I. F.; Sleight, A. W. *Acta Crystallogr. B* **1999**, *55*, 333−340.
(4) David, W. I. F.; Evans, J. S. O.; Sleight, A. W. *Europhys. Lett.* **1999**, *46*, 661−669.
(5) Wang, K.; Reeber, R. R. *Appl. Phys. Lett.* **2000**, *76*, 2203−2204.
(6) Auray, M.; Quarton, M.; Leblanc, M. *Acta Crystallogr. C* **1995**, *51*, 2210−2213.
(7) Allen, S.; Evans, J. S. O. *J. Mater. Chem.* **2004**, *14*, 151−156.
(8) Evans, J. S. O.; Hanson, P. A.; Ibberson, R. M.; Kameswari, U.; Duan, N.; Sleight, A. W. *J. Am. Chem. Soc.* **2000**, *122*, 8694−8699.
(9) Boivin, J.-C. *Int. J. Inorg. Mater.* **2001**, *3*, 1261−1266.
(10) Chou, F. C.; Johnston, D. C. *Phys. Rev. B: Condens. Matter* **1996**, *54*, 572−583.
(11) Reyes, A. P.; Hammel, P. C.; Ahrens, E. T.; Thompson, J. D.; Canfield, P. C.; Fisk, Z.; Schirber, J. E. *J. Phys. Chem. Solids* **1993**, *54*, 1393−1402.
(12) Kappesser, B.; Wipf, H.; Kremer, R. K. *J. Low Temp. Phys.* **1996**, *105*, 1481−1486.
(13) Bassat, J. M.; Odier, P.; Villesuzanne, A.; Marin, C.; Pouchard, M. *Solid State Ionics* **2004**, *167*, 341−347.
(14) Tranquada, J. M.; Kong, Y.; Lorenzo, J. E.; Buttrey, D. J.; Rice, D. E.; Sachan, V. *Phys. Rev. B: Condens. Matter* **1994**, *50*, 6340−6351.
(15) Mackenzie, K. J. D.; Smith, M. E. In *Multinuclear solid-state NMR of inorganic materials*; Chan, R. W., Ed.; Pergamon: Oxford, 2002; pp 333−395.
(16) Bastow, T. J.; Dirken, P. J.; Smith, M. E.; Whitfield, H. J. *J. Phys. Chem.* **1996**, *100*, 18539−18545.
(17) Adler, S. B.; Reimer, J. A.; Baltisberger, J.; Werner, U. *J. Am. Chem. Soc.* **1994**, *116*, 675−681.
(18) Emery, J.; Massiot, D.; Lacorre, P.; Laligant, Y.; Conder, K. *Magn. Reson. Chem.* **2005**, *43*, 366−371.
(19) Kim, N.; Grey, C. P. *Science* **2002**, *297*, 1317−1320.
(20) Kim, N.; Vannier, R. N.; Grey, C. P. *Chem. Mater.* **2005**, *17*, 1952−1958.
(21) Kristensen, J. H.; Farnan, I. *J. Chem. Phys.* **2001**, *114*, 9608−9624.

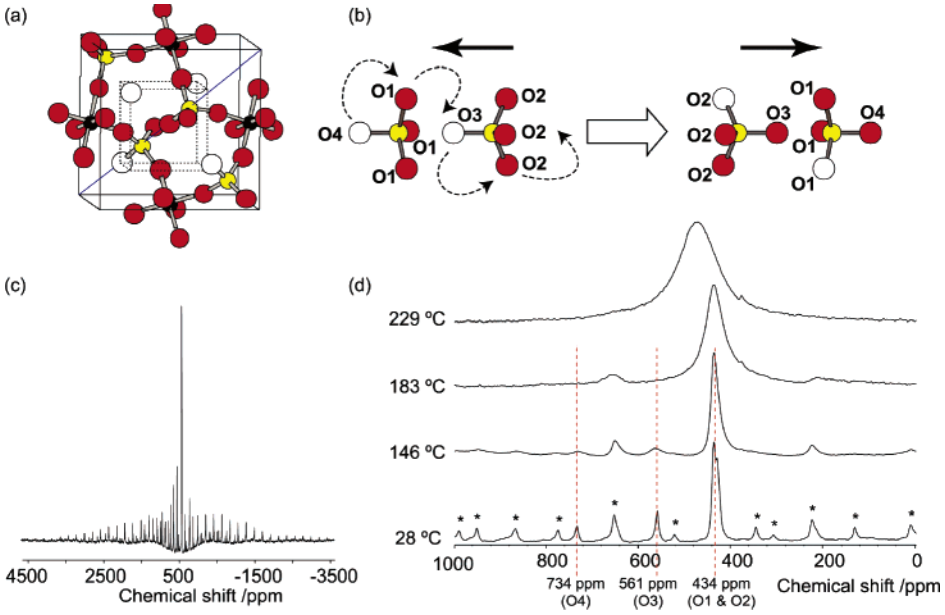

Figure 1. (a) Ball-and-stick representation of the structure of cubic ZrW_2O_8, showing two-coordinate oxygen sites (O1−3) in red, one-coordinate sites (O4) in white, zirconium atoms in black, and tungsten in yellow. (b) Schematic diagram showing the reversal of the W_2O_8 group direction (indicated by solid black arrows) by a "ratcheting" oxygen exchange motion. (c) ^{17}O magic-angle-spinning NMR spectrum of ZrW_2O_8 at 57 °C, showing the full spinning sideband manifold. (d) Representative ^{17}O MAS NMR spectra of ZrW_2O_8, illustrating the broadening of the resonances due to exchange as the temperature increases and their eventual coalescence into a single resonance. Asterisks denote spinning sidebands. See ref 22 for further experimental details.

zirconium tungstate, ^{17}O NMR shows unambiguously that the disorder is dynamic: all oxygen sites are in exchange. Moreover, as shown in Figure 1d, it clearly shows evidence for dynamics (via peak broadening) in the low-temperature phase. We have recently used two-dimensional exchange spectroscopy (EXSY) to show that full scrambling of the oxygen sites occurs at temperatures well below the α/β phase transition, suggesting a ratcheting mechanism for oxygen exchange, as shown in Figure 1b.[22] In this article, we show that these qualitative studies can be developed quantitatively to provide good estimates of the rate of oxygen exchange over a wide temperature range, hence allowing activation barriers for the motion in both phases to be derived. Models that reconcile the observation of significant motion in the low-temperature phase by NMR with the apparently fully ordered structure observed by diffraction are presented, together with evidence that strongly supports a model of transient fluctuations that increase in frequency as the phase transition is approached. We demonstrate that harmonization of the complementary information from diffraction and solid-state NMR studies provides a comprehensive understanding of the oxygen dynamics in this framework material.

Methodology

The NMR of spin-$^1/_2$ nuclei, such as ^1H and ^{31}P, is a powerful tool for the characterization of molecular dynamics. As explained below, however, the study of dynamics using "quadrupolar" spins ($I > {}^1/_2$) is significantly more complicated, with the notable exception of nuclei with small nuclear quadrupole moments, such as ^2H and ^6Li.[23,24] Unfortunately, the only potentially accessible spin-$^1/_2$ nucleus in zirconium tungstate is ^{183}W, which has very low receptivity (5 orders of magnitude lower than ^1H at natural abundance) and long relaxation times. Although we have been able to obtain an NMR signal from ^{183}W, the time required for even a simple NMR spectrum (65 h) made detailed investigations by ^{183}W NMR impractical. In contrast, we have previously demonstrated that ^{17}O ($I = {}^5/_2$) NMR of isotopically enriched samples provides direct qualitative information on the dynamic processes in this system. We now examine whether the NMR of half-integer quadrupoles (i.e., nuclei with spin quantum numbers of $^3/_2$,$^5/_2$, ...) can be used to provide quantitative information on dynamics in solids.

Particularly in the solid state, the NMR of nuclei with spin quantum numbers $> {}^1/_2$ is dominated by the coupling of the nuclear electric quadrupole moment with electric field gradients at the nucleus. In highly symmetrical environments, the quadrupole coupling, C_Q, may be small compared to the radio frequency used to excite the NMR coherences. In this case, the conventional vector model used to describe NMR of spin-$^1/_2$ nuclei can be applied without difficulty. More usually, however, the quadrupole couplings are several MHz in strength, leading to significant perturbation of the nuclear spin energies. The frequency of the central transition ($m_I = +{}^1/_2 \leftrightarrow m_I = -{}^1/_2$) is unaffected to first order by the quadrupole interaction, but the other NMR-allowed transitions (the "satellite" transitions) are strongly shifted. These orientation-dependent shifts may be sufficiently large (several MHz) that they cannot be readily excited with typical rf field strengths. Indeed, "soft pulse" excitation can then be used to selectively excite the central transition, which can be treated as a pseudo-spin-$^1/_2$.

The ^{17}O quadrupole couplings in ZrW_2O_8 fall between these limiting cases (an approximate value of $C_Q = 0.5$ MHz was obtained by fitting the well-resolved spinning sideband pattern of the O3 peaks in a 1D spectrum obtained at 40 °C). As a result, rf pulses excite significant intensity in the satellite transitions, which gives rise to spinning sideband manifolds in magic-angle-spinning (MAS) spectra, as seen in a typical spectrum for ZrW_2O_8 in Figure 1c.

The evolution of the NMR coherences under the simultaneous effects of motional exchange and spin−lattice relaxation, T_1, is somewhat complex and is presented here only in summary. A full treatment will be given elsewhere.[25] In general, the spin−lattice relaxation for an

(22) Hampson, M. R.; Hodgkinson, P.; Evans, J. S. O.; Harris, R. K.; King, I. J.; Allen, S.; Fayon, F. *Chem. Commun.* **2004**, 392−393.
(23) Schmidt-Rohr, K.; Spiess, H. W. In *Multidimensional solid-state NMR and polymers*; Academic Press: New York, 1994.
(24) Nagel, R.; Gross, T. W.; Günther, H.; Lutz, H. D. *J. Solid State. Chem.* **2002**, *165*, 303−311.
(25) Hampson, M. R.; Hodgkinson, P., submitted to *Solid State Nucl. Magn. Reson.*

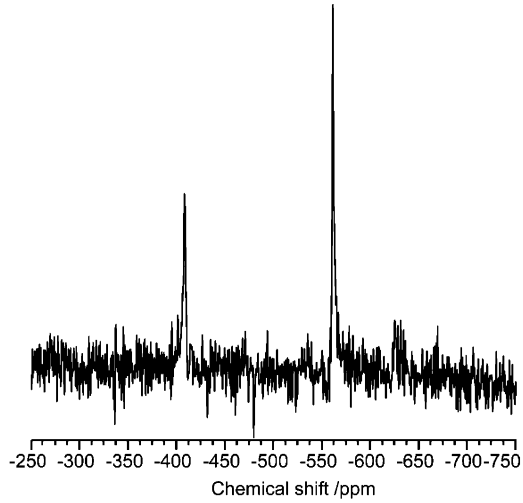

Figure 2. ^{183}W NMR spectrum of ZrW_2O_8 at ambient temperature. An excitation pulse duration of 3.6 μs (30°) and pulse delay of 70 s were used. The MAS rate was 4.5 kHz. 3360 transients were recorded in a total time of 65.3 h. The chemical shift was referenced to an aqueous solution of Na_2WO_4 at 0 ppm.

individual site is described by the relaxation matrix **R**, with an individual element $R_{m,m'}$ giving the rate of transfer from coherence m (e.g., $m_I = {}^1/_2$) to m' (e.g., $m_I = {}^3/_2$). The site exchange is described by the kinetic matrix **K** where k_{ij} is the rate of exchange of site i to site j. The combined exchange and relaxation can then be described in a direct-product Liouville space with the Liouvillian $\mathbf{L} = \mathbf{K} \otimes \mathbf{R}$.

Considering the site exchange in ZrW_2O_8 illustrated in Figure 1b, the kinetic exchange matrix for O1 ↔ O3 and O2 ↔ O4 is given by

$$\mathbf{K} = \begin{array}{c} \\ \text{O1/2} \\ \text{O3} \\ \text{O4} \end{array} \begin{array}{c} \begin{array}{ccc} \text{O1/2} & \text{O3} & \text{O4} \end{array} \\ \begin{pmatrix} -2k & k & k \\ k & -k & 0 \\ k & 0 & -k \end{pmatrix} \end{array}$$

Note that the O1 and O2 sites are not resolved (Figure 1d), and so we can only consider the total O1 and O2 magnetization, $M_{O1/2}$. It can then be shown that the evolution of the O1/2 magnetization under the influence of the exchange is given by $M_{O1/2}(t) = \alpha + \beta e^{-3kt}$, where the coefficients depend on the eigenvectors of **K** and the initial magnetizations. Detailed studies of spin−lattice relaxation have shown[25] that it can be described by a triexponential process with rate constants in the ratio $2W$:$12W$:$30W$ (corresponding to a dominant "magnetic" relaxation mechanism, in which ^{17}O relaxation is driven by the motion of neighboring ^{17}O spins). The rate process associated with the relaxation of the central transition, $2W$, is dominant and can be identified with the spin−lattice relaxation rate, $R_1 = 1/T_1$. The overall evolution under both relaxation and exchange is thus potentially the sum of six exponential decays, $2W$, $12W$, $30W$ and $3k + 2W$, $3k + 12W$, $3k + 30W$.

The difficulties of fitting complex multiexponential dynamics introduce considerable uncertainty into the absolute values of fitted rates.[25] As shown below, however, once we have established an estimated absolute rate of exchange at a single temperature, we can use straightforward measurements of the spin−lattice relaxation rate to determine the rate at any other temperature.

Experiments and Results

All NMR experiments were carried out using a Varian InfinityPlus spectrometer with an 11.7 T magnet, giving a frequency of 20.82 MHz for ^{183}W and 67.8 MHz for ^{17}O.

Figure 2 shows the ambient-temperature ^{183}W NMR spectrum of a sample of ZrW_2O_8 prepared by standard solid-state

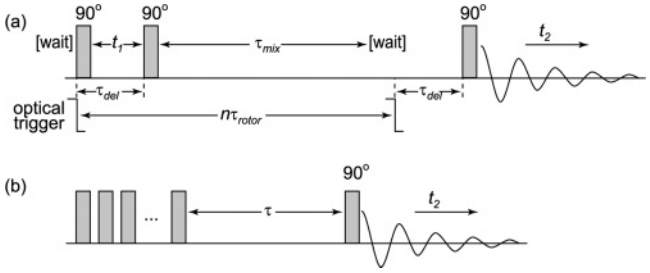

Figure 3. Pulse sequences used: (a) rotor-synchronized EXSY and (b) saturation recovery. Quantitation of the EXSY results is only possible if 90° pulses bracketing the mixing time occur at the same point in the rotor cycle. The sequence is triggered by an optical signal from the rotor, and the triggering of the final 90° pulse is delayed in order to achieve this synchronization. Note that the diagram is not to scale, and this additional delay is negligible in comparison to τ_{mix}.

methods[26] and packed into a 7.5 mm zirconia MAS rotor. This shows two resonances at −408 and −561 ppm, as would be expected from the crystal structure.[1,6] However, due to the low receptivity of ^{183}W, and despite a total experiment time of 65 h, the signal-to-noise ratio is extremely poor. ^{183}W NMR is clearly unsuitable for detailed quantitative studies, and we have used ^{17}O NMR to characterize the dynamics in this material.

An isotopically enriched sample of ZrW_2O_8 was used for all ^{17}O NMR experiments. This was prepared via the hydrated $ZrW_2O_8{\cdot}xH_2O$ phase[27] by hydration of ZrW_2O_8 with 40% ^{17}O-enriched water followed by dehydration. This technique produced a highly enriched and pure sample of ZrW_2O_8 and is considerably more effective than earlier attempts starting from the pre-enriched binary oxides.[28] Although it is difficult to determine experimentally the level of isotopic enrichment, a theoretical maximum ^{17}O abundance of about 30% may be estimated on the assumption of a statistical scrambling of oxygen atoms between the enriched water and the starting material. ^{17}O chemical shifts were referenced to the signal from $H_2{}^{17}O$ (natural abundance) at 0 ppm. The sample was packed in a 4 mm zirconia MAS rotor and spun at a rate of 14.5 kHz, actively maintained to within 5 Hz by an automated spin rate controller. The duration of the nominal 90° pulses was optimized on the sample and determined to be ∼1.9 μs. Temperatures were calibrated using the chemical shift of the ^{207}Pb NMR signal of $Pb(NO_3)_2$,[29] with an observed temperature gradient across the sample of approximately 10 °C.

The 2D EXSY experiments we recorded for qualitative studies require about 38 h of spectrometer time.[22] Hence following the kinetics of oxygen exchange by observing the redistribution of magnetization in a 2D EXSY as a function of the mixing time, τ_{mix}, would be unfeasibly time-consuming. As the nature of the exchange has been qualitatively determined, however, a simpler one-dimensional version of EXSY can be used. In solution-state NMR this would normally be done using selective inversion pulses to create nonequilibrium magnetization at the site of interest. Since such pulses would be ineffective in the presence of significant quadrupole couplings, the normal three-pulse EXSY sequence was retained (Figure 3a), but a fixed

(26) Chang, L. L. Y.; Scroger, M. G.; Phillips, B. *J. Am. Ceram. Soc.* **1967**, 211−215.
(27) Duan, N.; Kameswari, U.; Sleight, A. W. *J. Am. Chem. Soc.* **1999**, *121*, 10432−10433.
(28) Hampson, M. R.; Allen, S.; King, I. J.; Crossland, C. J.; Hodgkinson, P.; Harris, R. K.; Fayon, F.; Evans, J. S. O. *Solid State Sci.* **2005**, *7*, 819−826.
(29) Bielecki, A.; Burum, D. P. *J. Magn. Reson.* **1995**, *116*, 215−220.

evolution time, t_1, was used to create the initial nonequilibrium state. The kinetics of the redistribution of magnetization can then be studied by varying τ_{mix}. Without careful synchronization of the mixing time to the sample rotation, the signal intensity is also a function of the difference in rotor phase at the start and end of the sequence, which would obscure the dependence on the exchange process. An optical signal from the rotor was therefore used to trigger the pulses, ensuring that the mixing time was always a multiple of rotation period.[30,31] As we are only interested in the exchange of centerband intensity, it was not necessary to modify the pulse sequence to obtain correctly phased line shapes for the sidebands.[31] The fact that the quadrupole couplings are neither much smaller nor much larger than the rf field strength (expressed as nutation rates) means that it is important to use such simple and robust experiments. Not only does the quadrupole coupling, and hence the behavior of the nuclear spin coherences when excited by rf, depend on the crystallite orientation with respect to the external field, but the effective quadrupole couplings are also modified by the oxygen dynamics (at sufficiently high exchange rates, the quadrupole coupling will be averaged to zero on the time scale of the NMR experiment by the rapid site exchange). As a result, it is difficult to predict the distribution of NMR coherences after pulsed excitation with much confidence. Hence in attempting to quantify the dynamics using ^{17}O NMR, it is necessary to use experiments that minimize the complicating effects of the quadrupole couplings.

EXSY experiments were carried out at a calibrated sample temperature of 110 °C. In each experiment, 40 values of the mixing time, in the range 10 μs to 50 s were used in order to capture the different rate processes due to exchange and T_1 relaxation. Unlike two-site exchange, where the transmitter frequency would generally be set midway between the two resonance, and the evolution time to $t_1 = 1/4\Delta$ (where Δ is the difference in NMR frequencies), there is not a natural choice of initial starting condition. Hence a number of different starting conditions were used, by varying the value of t_1 and the transmitter frequency within the spectrum.

The saturation recovery experiment, Figure 3b, was used to determine the T_1 relaxation behavior over the temperature range 40−226 °C. In this experiment, a large number of pulses (typically 100) are used to saturate the magnetization, followed by a single read pulse after a delay time, τ. This experiment is particularly useful for measuring long T_1 values, since the initial saturation avoids the need for full magnetization recovery before repeating the experiment.

After suitable processing to maximize the signal-to-noise ratio ("matched filtering" with a 900 Hz Lorentzian line-broadening), the heights of the centerbands were extracted as a function of τ_{mix}. Ideally we would simultaneously fit the resulting curves of intensity vs time from each of the centerbands. However, only the data from the strong overlapped O1/O2 signals had sufficient intensity for reliable quantitative analysis, and the lower-quality data sets obtained from the other sites were discarded. Figure 4a shows a typical data set, with the logarithmic plot revealing the presence of at least three exponential processes in the overall decay of the signal as a function of τ_{mix}. In principle, we are expecting six components, at $2W$, $12W$, $30W$ and $3k + 2W$, $3k + 12W$, $3k + 30W$. The slowest component can be identified with the $2W$ spin−lattice relaxation process. As seen in Figure 4a, $k \gg W$, and so we are not able to distinguish the three components that involve both k and W; thus, we simply identify the fastest process in the EXSY curve with the exchange. (This fast initial decay is not observed in the pure relaxation studies.) Unfortunately we cannot hope to fit more than three independent processes, particularly as the coefficients of the different components must be left free, as we cannot determine the initial populations of the different coherences with any accuracy. Hence we simply fit the EXSY data to three exponential decays, with rate constants, k_1, k_2, and k_3, identifying k_1 with the site exchange ($3k$) and k_3 with the dominant component of the T_1 relaxation and leaving the precise nature of k_2 undetermined.

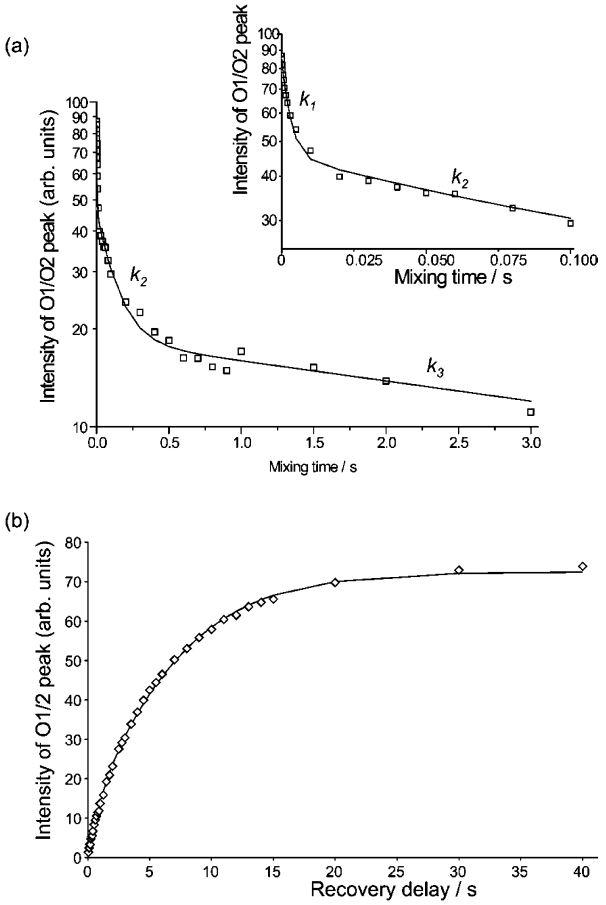

Figure 4. Representative data sets and fitting from (a) 1D EXSY at 110 °C ($t_1 = 58$ μs, 32 transients per data point, recovery period of 30 s between transients) and (b) saturation recovery at 110 °C. The plots show the intensity of the O1/O2 peak as a function of mixing/recovery time.

As a consequence of the difficulty of modeling such complex exchange plus relaxation behavior, the fitted values are subject to significant distortion. This can be seen in Figure 5, which plots the resulting k_1 and k_2 from a number of experiments performed at the same temperature, varying only in the initial EXSY starting conditions. Reassuringly, the results from repeat experiments using identical initial conditions are clustered within the error bars of the fitting. Varying the starting conditions, however, has a significant effect on the fitted parameters, which indicates that systematic errors are more significant than the estimated error bars imply. We can, however, make a conserva-

(30) de Jong, A. F.; Kentgens, A. P. M.; Veeman, W. S. *Chem. Phys. Lett.* **1984**, *109*, 337−342.
(31) Hagemayer, A.; Schmidt-Rohr, K.; Spiess, H. W. *Adv. Magn. Reson.* **1989**, *13*, 85−130.

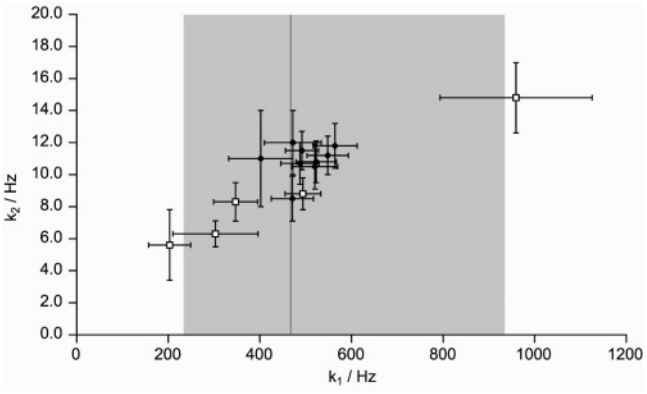

Figure 5. Scatter plot of rate constants k_1 against k_2 fitted from 1D-EXSY experiments at $T = 110$ °C. Closed points correspond to experiments with the same initial conditions ($t_1 = 58$ μs, transmitter frequency set to the O1/O2 peak frequency); open data points correspond to a variety of other initial conditions. The solid line and shaded area represent the average value and estimated error range for k_1, respectively (see text for details).

tive estimate of the underlying exchange rate. Replacing data points acquired with identical starting conditions with mean values and then taking the mean of the resulting six data points gives an average k_1 of 467 Hz (solid vertical line). The shaded area in Figure 5 indicates the estimated uncertainty in k_1, assuming that the true exchange rate lies within a range of a factor of 2 smaller or greater than the estimated value. Hence the exchange rate at 110 °C, $k_{exch} = k_1/3$, is estimated to be 160 Hz within a range of 80−310 Hz (figures to 2 s.f.). Expressing the uncertainty in this fashion leads to a well-defined error bar in ln k_{exch} (cf. Figure 6).

In principle, the uncertainty could be reduced by elaborating the model to include data from the O3 and O4 sites. However, a complete model of the process that attempted to include excitation efficiencies and finite pulse effects (i.e., evolution under the quadrupole interactions during the rf pulses) would be extremely complex and would require detailed information about the quadrupole interactions and how these are modulated by the motion. Given the intrinsically low sensitivity of ^{17}O solid-state NMR, it is doubtful that uncertainties could be reduced sufficiently to justify the considerable effort involved. Despite the relatively large uncertainties, these results are the first quantitative measurements of slow oxygen exchange in such materials. Moreover, as shown below, the determination of *relative* rates (and related quantities, such as activation barriers) is unaffected by the uncertainties in the absolute rate constants.

The T_1 relaxation was quantified from the O1/O2 peak of the saturation recovery data sets. Since the site exchange is always faster than the T_1 relaxation, the observed relaxation decays should be the same for all sites. The curves were fitted to a triexponential, but now the relative values of the rate constants could be fixed (in the ratio 2:12:30), reducing the fitting parameters to a single rate value and three amplitude coefficients. Such fits are considerably more robust than those for the EXSY, as can be seen in Figure 4b. The slowest component (corresponding to the 2W process in the analysis above) was always dominant and is identified with the basic spin−lattice relaxation rate, R_1 ($1/T_1$). Above 180 °C, the different oxygen sites are not resolved, and so the integrated intensity of the broad coalesced peak was used, with the data

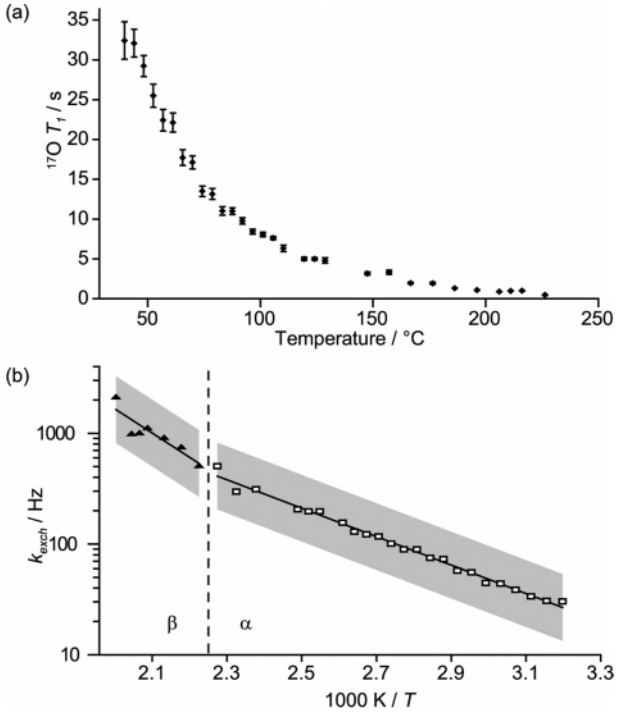

Figure 6. (a) Fitted ^{17}O T_1 values as a function of temperature, (b) calculated k_{exch} vs inverse temperature; the gradients of the fitted straight lines give the activation energy above and below the phase transition (solid and open points, respectively). The uncertainty in the absolute values in k_{exch} means that the true data points are estimated to lie within the shaded region (which corresponds to that of Figure 5), but does not affect the value of the activation energy.

Table 1. Arrhenius Parameters Derived from Fitting Temperature Dependence of k_{exch} to ln $k_{exch} = A - E_a/RT$

	E_a/kJ mol^{-1}	log (A/s^{-1})
α phase	24.5 ± 0.5	5.5 ± 0.1
β phase	42 ± 9	7 ± 1

fitting well to a single exponential. Full details of the relaxation model and analysis can be found in an accompanying publication.[25]

The proposition that the T_1 relaxation is a strong function of the motional exchange is confirmed by Figure 6a, which shows that T_1 drops from 32 s at 40 °C to 0.5 s at 226 °C. The relaxation rate is proportional to the spectral density at the ^{17}O NMR frequency, $J(\nu_{NMR})$,[32] which is in turn proportional to the jump rate if the relaxation is indeed being driven by the reorientation of the W_2O_8 units. The constant of proportionality can then be determined from the estimate of k_{exch} at 110 °C derived from the EXSY experiments, allowing the T_1 values to be converted to exchange rates. Figure 6b plots the resulting k_{exch} values as a function of inverse temperature. The plot shows two linear sections, with a clear discontinuity in the gradient around the α/β phase transition at 175 °C; that is, we can extract distinct activation barriers for the oxygen exchange above and below the phase transition. These are given in Table 1. There is no measurable discontinuity in the k_{exch} values themselves, confirming the second-order nature of the transition. This coincides with earlier qualitative work[22] in which a smooth variation in the ^{17}O NMR spectra through the phase transition was observed.

(32) Harris, R. K. In *Nuclear Magnetic Resonance Spectroscopy*; Longman: Harlow, U.K., 1983.

It is also important to note that the difficulties in quantifying the EXSY data affect only the *absolute* rate constants (and the pre-exponential factor, A). Since the activation barriers are derived from the gradient of plots of ln k_{exch} vs $1/T$, the relatively large error in the proportionality constant is not significant. The accuracy of the activation barriers is essentially determined by the fitting of the saturation recovery data, which is considerably more robust, as indicated by the quality of the linear fits in Figure 6b. The errors on E_a shown in Table 1 show the statistical errors associated with the linear regressions. The relatively high error on the estimate for the high-temperature phase is a consequence of the limited temperature range over which measurements could be made.

We can test whether the estimated rate constants extrapolated from the low-temperature EXSY results are consistent with previously observed NMR spectra by calculating the exchange rate at high temperature, when the signals from the different oxygen sites have "coalesced" (about 200−250 °C). The value of $k_1 = 3k_{exch}$ in this region, calculated using the fitted Arrhenius parameters from Table 1, is in the region of 3−8 kHz, which is consistent with the differences in ^{17}O NMR frequencies at the magnetic field used (e.g., 9 kHz between O1/2 and O3). This confirms that the T_1 values are indeed directly related to the exchange process quantified by the EXSY experiments.

These results are in good agreement with isolated results obtained using different techniques. At high temperatures, dielectric measurements on ZrW_2O_8 gave an estimated activation barrier for oxygen exchange of 0.50 eV (48 kJ mol^{-1}) between ~500 and 800 K for ZrW_2O_8.[2] Time-dependent powder diffraction studies have provided rate estimates in the low-temperature phases of related materials. A series of time-dependent experiments on a quenched sample of $ZrWMoO_8$ gave an activation energy of 34 ± 5 kJ mol^{-1} for $ZrWMoO_8$ between 205 and 230 K.[7]

Discussion

The measurements of ^{17}O exchange rate clearly show that the reorientation of the W_2O_8 units, illustrated in Figure 1b, occurs over the complete temperature range studied. There is only a small, but distinct, difference in the activation barrier on either side of the α/β phase transition. This is consistent with the simple one-dimensional ^{17}O spectra that evolve smoothly from the "slow exchange" regime below the phase transition to fast exchange above, with no obvious discontinuity at the transition (Figure 1d). At first sight, however, this appears inconsistent with earlier diffraction studies that indicate that the low-temperature phase is essentially fully ordered.

Figure 7 presents two possible models which allow the NMR and X-ray data to be reconciled. Figure 7a represents a situation in which large domains within the material undergo concerted flips of the W_2O_8 groups. Assuming the time scale of the inversion process is short relative to that of a typical diffraction data collection (on the order of minutes), and the domain size is large (>~1000 Å), then diffraction experiments will report a fully ordered material, whereas NMR magnetization exchange experiments will report dynamic disorder.

A second, more plausible model is shown in Figure 7b. In this scenario, local flips of W_2O_8 groups occur at low temperature within an essentially ordered domain. Provided the concentration of such groups is low, they would not cause

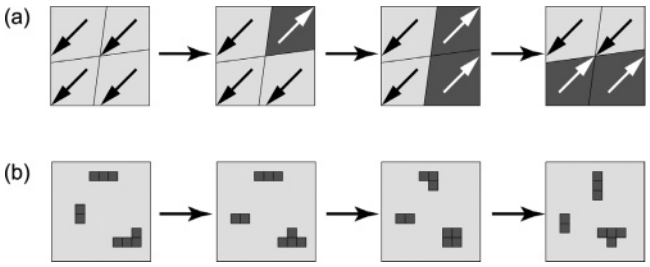

Figure 7. Schematic illustration of proposed limiting models for W_2O_8 inversion in the low-temperature phase of ZrW_2O_8: (a) domains, which are large on the diffraction length scale, that reverse orientation (represented by arrows) and (b) ordered domains containing low concentrations of "reversed" units (darker squares). Note that domain orientations correspond to the W_2O_8 unit orientations as shown in Figure 1b. Both models are consistent with the observation of high ordering from diffraction studies, but continued inversion at low temperatures from NMR.

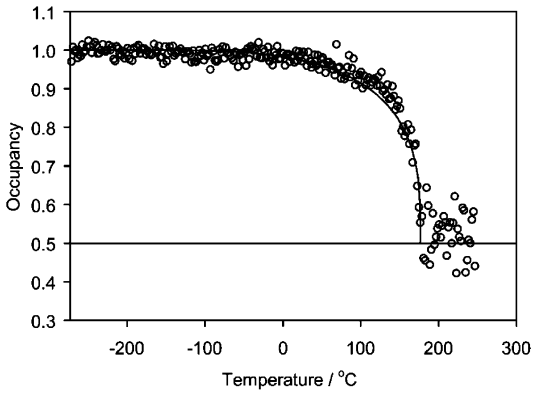

Figure 8. Fractional site occupancy of the major W_2O_8 orientation as a function of temperature. The solid line is a fit to a three-dimensional cubic Ising model (see text). Figure adapted from ref 3.

significant changes in either peak intensities or reflection peak widths (which reflect, inter alia, the size of ordered domains in a material) in a powder diffraction pattern. Fluctuations involving short-lived or moving local "islands of disorder" (possibly individual W_2O_8 units) could then occur within the time frame of a diffraction experiment such that NMR reports a material in which the oxygens are in dynamic exchange, whereas diffraction methods report an ordered material. Note that this model requires that the rate at which units (or islands) realign with the surrounding domain or migrate through it exceed the rate at which they jump out of alignment (otherwise the long-time equilibrium state would be a fully disordered structure). As the temperature of the system is raised, the concentration and size of the "flipped" regions grow until the point where the number of "flipped" and "unflipped" groups becomes comparable and one has the time-averaged $Pa\bar{3}$ structural model. Diffraction data support such a structural evolution in a number of ways. First there is a gradual decrease in the order parameter as a function of temperature, as shown in Figure 8. Treating the W_2O_8 orientation as formally equivalent to the magnetic dipole of a spin-$^1/_2$ nucleus, this disordering process can be described in terms of a three-dimensional Ising model (with essentially no adjustable parameters).[3] The fit to a cooperative model of the ordering strongly supports the hypothesis that a jump out of alignment creates strain. An examination of the ($h0l$, $h \neq 2n$) reflections, which are characteristic of the ordering process, provides further support for moving flipped domains

within the material. These peaks show no significant broadening relative to other reflections as one approaches the phase transition, suggesting a single characteristic length scale for diffraction throughout the material. A model such as Figure 7a in which the phase transition involved the flipping of diffraction-coherent domains whose size decreases as the phase transition is approached would be expected to cause broadening of the ordering peaks.

It is important to note the important complementary role played by the diffraction studies at this point. The NMR magnetization transfer experiments cannot distinguish between these two motional models, as their kinetic exchange matrices are identical. If we construct the kinetic exchange matrix for two successive jumps, then it is identical (within a scaling factor) to the matrix for a single jump and is independent of whether the averages times between the "forward" and "reverse" jumps are the same ("domain" model) or significantly different ("fluctuation" model). Similarly, motion that does not lead to re-labelling of the sites will not be detected by magnetization transfer (although it may be detectable in relaxation studies). If, for instance, we assume that the fluctuation model is appropriate, but that "flipped" unit returns to *exactly the same configuration* (i.e., initial O3 sites finish as O3, etc.), then this motion will not contribute to magnetization transfer. However, such strongly non-Markovian behavior is highly implausible, particularly given the direct relationship between T_1 relaxation and site exchange.

Conclusions

^{17}O NMR is shown to be a powerful complement to diffraction methods for the study of this material, with particular strength in the characterization of dynamics. Although the quantitative use of ^{17}O solid-state NMR is significantly more complex than for spin-$^1/_2$ nuclei, it is nevertheless feasible to extract reasonable estimates of exchange rates from magnetization transfer experiments. These can then be extrapolated by straightforward measurements of NMR relaxation times to determine exchange rates and robust values of activation barriers over a wide temperature range. The strategy of working at relatively low dynamic exchange rates in order to characterize the nature of oxygen exchange should be widely applicable to other systems in which individual ^{17}O sites are resolved.

The different pictures provided by NMR and diffraction methods (resulting from their different time scales) strongly constrain the range of models that can simultaneously explain both sets of data. This has allowed us to propose a comprehensive model for the oxygen motion in cubic ZrW_2O_8, and we are now extending these studies to related materials.

Supporting Information Available: Figure showing fitting of spinning sideband pattern of ^{17}O NMR spectrum to obtain C_Q estimate (PDF). This material is available free of charge via the Internet at http://pubs.acs.org.

JA054063Z